Applied Surface Science 353 (2015) 588–593

Contents lists available at ScienceDirect

Applied Surface Science

journal homepage: www.elsevier.com/locate/apsusc

As_4 overpressure effects on the phase purity of cubic GaN layers grown on GaAs substrates by RF-MBE

Y.L. Casallas-Moreno[a,*], S. Gallardo-Hernández[a], F. Ruiz-Zepeda[b], B.M. Monroy[c], A. Hernández-Hernández[d], A. Herrera-Gómez[e], A. Escobosa-Echavarría[f], G. Santana[c], A. Ponce[b], M. López-López[a]

[a] Physics Department, Centro de Investigación y de Estudios Avanzados del IPN, Apartado Postal 14-740, 07000 México D.F., Mexico
[b] Department of Physics and Astronomy, University of Texas at San Antonio, San Antonio, TX 78249, United states
[c] Instituto de Investigaciones en Materiales, Universidad Nacional Autónoma de México, Apartado Postal 70-360, Coyoacán, 04510 México D.F., Mexico
[d] Escuela Superior de Apan, Universidad Autónoma del Estado de Hidalgo, Calle Ejido de Chimalpa Tlalayote, 43990 Apan, Hidalgo, Mexico
[e] Centro de Investigación y de Estudios Avanzados del IPN, Unidad Queretaro, 76230 Queretaro, Mexico
[f] Electric Engineering Department, Centro de Investigación y de Estudios Avanzados del IPN, Apartado Postal 14-740, 07000 México D.F., Mexico

ARTICLE INFO

Article history:
Received 12 March 2015
Received in revised form 1 June 2015
Accepted 9 June 2015
Available online 18 June 2015

Keywords:
Cubic GaN
As_4 overpressure
Relaxation process
Nucleating layer
Stacking faults
RF-MBE

ABSTRACT

Cubic GaN samples on GaAs(0 0 1) substrates were grown by RF-plasma-assisted molecular beam epitaxy (RF-MBE), an As_4 overpressure was employed during the nucleating layer. We found that the relaxation process of c-GaN during the nucleating layer, affects the purity of cubic phase. Higher cubic phase of GaN was obtained for samples that initiated the relaxation process after some monolayers (8ML) of growth, as a result of better stabilization of the cubic layer. The relaxation process depends on the As_4 overpressure over the growth surface and on the growth temperature. The structural properties of c-GaN characterized by transmission electron microscopy (TEM) and high resolution X-ray diffraction (HR-XRD) have evidenced the purity of cubic phase in the first nanometer of growth, and also the formation of the hexagonal inclusions after several nanometers of growth from the stacking faults on the {1 1 1} planes. From an estimation of the hexagonal content by X-ray reciprocal space mapping (RSM), we found a lower hexagonal component on the $(1\,\bar{1}\,1)_N$ and $(\bar{1}11)_N$ planes. The highest purity of cubic GaN was 98.7% along the $\{1\,1\,1\}_N$ planes for sample grown at 720°C. Photoluminescence measurements also demonstrated the high purity of the cubic phase of this sample, no emission of hexagonal inclusion was detected.

1. Introduction

Gallium nitride (GaN) and its alloys are important materials for developing optoelectronic and electronic devices. This is mainly due to their outstanding properties such as the direct energy gap, which covers a large part of the solar spectrum, from the infrared to the ultraviolet. Moreover, devices based on these materials can be operated at higher power, frequency, and reliability. All these features in hostile environments with a lower energy consumption [1]. GaN can be synthesized in two crystalline structures: hexagonal and cubic [2]. In comparison to the widely employed stable hexagonal phase of GaN (h-GaN), the metastable cubic one (c-GaN) presents remarkable advantages [3]. Because of its high degree of crystallographic symmetry, one of the most important advantages is that effectively eliminate the spontaneous polarization and strong piezoelectric fields [4]. Besides, the cubic phase presents a high mobility of carriers, the ease to get p-type doping and, more suitable cleaving planes [5–7].

One of the major difficulties for obtaining high quality c-GaN is the absence of lattice-matched substrates. Nevertheless, an extensive investigation in recent years has resulted in the successful growth of c-GaN on different substrates such as Si, SiC, MgO, as well as on GaAs [8–12]. In this process, the nucleating layer was identified as a key factor to overcome the lattice mismatch and to reduce the hexagonal inclusions. Efforts have been made to control the growth of this layer. For instance, it was proposed a nucleating layer deposited at a low temperature prior to GaN epitaxial growth at a high temperature [13], and also to employ an Arsenic (As_4) overpressure during the nucleating layer to induce the cubic growth over GaAs substrates. In this last process was found that the content of c-GaN increases, by increasing the growth temperature at 700°C, with a flux of arsenic at 2.4×10^{-7}Torr [14]. The analysis by reflection high-energy electron diffraction (RHEED) for this layer

* Corresponding author. Tel.: +1 00525536650130.

http://dx.doi.org/10.1016/j.apsusc.2015.06.054
0169-4332/

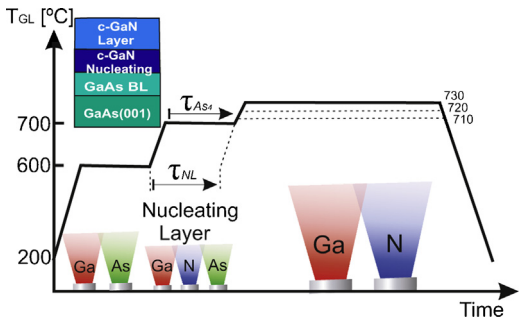

Fig. 1. Schematic representation of the different stages of growth of c-GaN films on GaAs(0 0 1).

showed, an initial (3×3) reconstruction during the growth of the first GaN monolayer [15]. However, is of great importance an understanding of the relaxation process of c-GaN during the nucleating layer, due to the impact on the final crystal quality.

In this work, we studied the effect of varying the exposure time to the As_4 overpressure during the nucleating layer on the relaxation process of c-GaN. We have found that the relaxation process is directly related with the purity of cubic phase. Under appropriate conditions a stable nucleating layer can be formed which promotes the cubic phase growth. Structural and optical characterization of c-GaN allowed us evaluate the purity of the cubic phase. In fact, the analysis by reciprocal space mapping (RSM) enabled us to obtain some fine details on the purity of cubic phase on the {1 1 1} planes. The $(\bar{1}11)_N$ and $(1\,\bar{1}\,1)_N$ planes present a higher purity of cubic phase compared with the $(1\,1\,1)_{Ga}$ and $(\bar{1}\,\bar{1}\,1)_{Ga}$ planes. We propose a mode to explain this difference.

2. Experimental details

c-GaN samples were grown in a Riber C21 RF-MBE system on semi-insulating GaAs(1 0 0) substrates. The system is equipped with a radio-frequency (RF) plasma source and effusion cells, for supplying reactive atomic nitrogen, and Ga and As fluxes, respectively. In order to prepare a smooth GaAs surface that helps the nucleation of c-GaN, the GaAs substrate was thermally cleaned, and then a 100nm-thick GaAs buffer layer was grown. The growth conditions were: growth temperature (T_G) of 600°C, a Ga beam equivalent pressure (BEP_{Ga}) of 5.3×10^{-7}Torr, and an As BEP_{As} of 8.3×10^{-7}Torr. A schematic of the growth process is illustrated in Fig. 1.

For the growth of the c-GaN nucleating layer, we used a growth temperature (T_{NL}) of 700°C during a time τ_{NL} of 18s, and a constant As_4 overpressure on the growth surface applied for a time (τ_{As_4}). The presence of As atoms allows the formation of a cubic template of GaAs. The As atoms of this template are replaced by N atoms, as a consequence of the higher bond energy of Ga—N compared to that corresponding to Ga—As bond. We shall discuss further this point in Section 3. Besides, with the purpose of evaluating the influence on the purity of cubic phase GaN, we tested different periods of time for As_4 overpressure exposure (τ_{As_4}). Finally, over the nucleating layer, c-GaN films were grown by varying the growth temperature (T_{GL}). The growth parameters of the samples are summarized in Table 1. The Nitrogen (N) plasma source during all growths was operated at 150W with a N_2 flow of 0.25sccm, and the Ga beam BEP_{Ga} set at 2.7×10^{-7}Torr.

The initial nucleation and subsequent growth of GaN films were monitored in-situ by using RHEED. The Ga—As and Ga—N bonds were determined by angle-resolved X-ray photo-electron spectroscopy (AR-XPS). A monochromatic Al Kα source with a photon energy of 1486.6eV was used. The atomic crystalline structure was characterized using high-resolution transmission electron

Table 1
Parameters of c-GaN samples.

Sample	τ_{As_4} [s]	T_{GL} [°C]	[a] τ_{II} [s]	[b] T [nm]	FWHM [arcmin]
I	3	720	4.5	371	83.84
II	180	720	22	378	81.34
III	180	710	25	377	93.96
IV	900	720	21	367	102.24
V	900	730	20	354	119.42
VI	30	700			

[a] τ_{II} is the time to reach stage II shown in Fig. 2.
[b] T is the thickness of the sample.

microscopy (HR-TEM) by a JEOL ARM 200F microscope operated at 200kV. The analyzed samples were prepared in cross-section by mechanical polishing. High resolution X-ray diffraction (HR-XRD) was performed in a Panalytical MRD X-ray diffractometer employing a Cu Kα source and a Ge(2 2 0) triple axis analyzer. Chemical composition of the material was analyzed by time of flight secondary ion mass spectrometry (TOF-SIMS) from IONTOF. Finally, optical characterization was obtained by photoluminescence spectroscopy. The PL spectra were collected using a cryostat to change the sample temperature from 10 to 300K, and a He-Cd laser of 325nm excitation wavelength with a maximum input power of 20mW.

3. Results and discussion

The c-GaN growth turns out to be very sensitive to the formation of polycrystalline material and incorporation of hexagonal phase, due to its metastable character, and the large lattice mismatch of 20% with the GaAs substrate. Therefore, to understand the growth mechanism and to improve the crystal quality of c-GaN, it is very important to study the early stages of formation of the nucleating layer. First, we analyzed the relaxation process of cubic GaN. The variation in the lattice constant ($\Delta a/a_0$) during the nucleation of GaN for sample I, is shown in Fig. 2. We observed an interesting oscillation of the lattice constant during the first stages of growth.

The GaN nucleating layer is initiated in the stage I of Fig. 2, with an As_4 overpressure. At this stage, the RHEED pattern of GaAs turns into a (3×3) pattern during the first 3s, that corresponds to the first strained c-GaN monolayer. In this monolayer, c-GaN is grown by replacing As by N in the cubic lattice of GaAs, which is an anion exchange reaction [16]. This reaction is a result of the higher bond energy of Ga—N (96.8kcal mol^{-1}) compared to Ga—As (47.7kcal mol^{-1}) [14]. Accordingly, GaN is forced to reproduce the cubic template.

The (3×3) reconstruction is a strained GaN monolayer almost fully N-terminated [14,16]. Following this monolayer, the transition to an unreconstructed (1×1) pattern was observed. With the

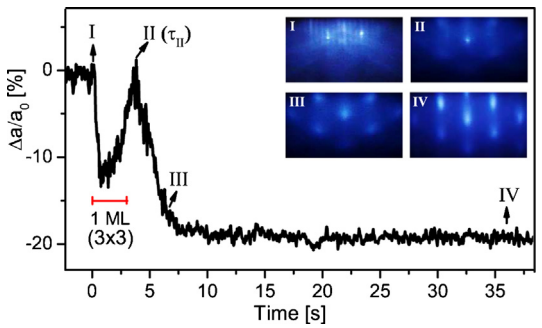

Fig. 2. Variation of in-plane lattice constant ($\Delta a/a_0$) during the nucleation of c-GaN and corresponding RHEED patterns. a_0 is the lattice constant of GaAs. The RHEED patterns were taken along [1 $\bar{1}$ 0] azimuth.

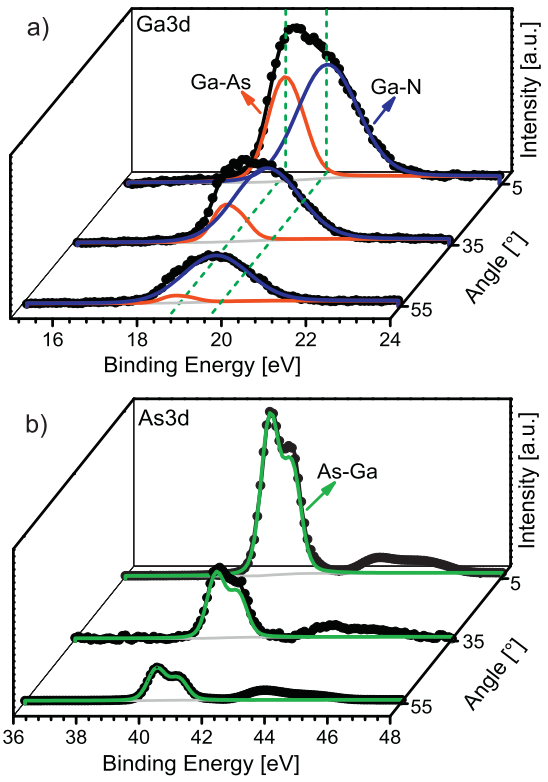

Fig. 3. XPS spectra of (a) Ga3d and (b) As3d for sample VI, grown at 700 °C.

presence of As on the growth surface, during the (1 × 1) pattern the formation of Ga—As bonds is again favored. As a consequence, the lattice constant increased. In fact, the lattice recovered the same value of that of GaAs, as shown in the stage II of Fig. 2. Immediately after, a decrease of the lattice constant was observed, suggesting the interchange of As by N atoms. Moreover, at this stage the full relaxation process of GaN is carried out, initiating the growth of c-GaN in a stable layer. The lattice constant in the stage IV corresponds to a relaxed c-GaN, with a bright and elongated RHEED pattern, thus indicating a smoothening of the growth front.

We noticed that the relaxation process of c-GaN, starting at stage II (τ_{II}), depends on the As content on the growth surface. In Table 1 we observe that with the shorter time of As_4 overpressure (τ_{As_4} = 3 s), the stage II is reached at τ_{II} = 4.5s (sample I). By increasing τ_{As_4} (samples II–V), τ_{II} also is increased, but is limited by the time of the nucleating layer (τ_{NL}), since we increased the growth temperature T_{GL} at τ_{NL} = 18s. The temperature increase promotes the desorption of As and Ga atoms from the growth surface, which results in that τ_{II} is reached around 22s, as shown in Table 1. τ_{II} = 22s is suitable to obtain a stable cubic layer. Employing higher growth temperatures (T_{GL}) after of the nucleating layer, the relaxation process (τ_{II}) starts faster (samples II–III and IV–V).

The RHEED analysis indicates that the As atoms are desorbed from the growth surface during the nucleating layer. In order to check the presence of As in the samples, we studied the chemical bonds in a nucleating layer of c-GaN by using angle resolved-XPS. Chemical analysis was performed for sample VI (with thickness of 3nm), at emission angles of 5°, 35° and 55°, which were taken with respect to the normal surface. Fig. 3 shows XPS spectra of (a) Ga3d, and (b) As3d. The Ga3d peak with the greatest analyzed depth (≈10nm), which corresponds to the emission angle of 5°, is composed of Ga—N bonding at the high-energy side, and Ga—As bonding at the low energy region [17]. In the most superficial analysis (≈5.5nm with an emission angle of 55°) of Ga3d, the peak is mainly composed Ga—N bonds, because in this case we are decreasing the contribution from the underlaying GaAs layer. Likewise, the intensity of As-Ga component in the spectra of As3d decreases with the decrease in the depth of analysis as observed in Fig. 3(b). The spectra taken from the nucleating layer of c-GaN showed evidence of the formation of Ga—N bonds during the first monolayers of growth, and the absence of Ga—As bonds on the growth surface. This latter point indicates that the As atoms are effectively desorbed from the surface.

In order to improve the growth of c-GaN on GaAs is convenient in the first place, to know the growth mechanism at the atomic scale. With this in mind, cross-sectional transmission electron microscopy (HR-TEM) was performed. Selected area electron diffraction (SAD) pattern in Fig. 4(a) shows a superposition of diffraction spots of c-GaN and GaAs buffer layer at the interface for sample IV. We observed from these patterns a perfect coherence on intensity and disposition of the diffraction spots. Thus, c-GaN has the same orientation of GaAs and the strain distribution due to the lattice mismatch is homogeneous within the layer of GaN [18]. The lattice constant obtained for GaN is a = 0.452nm, from the distances between the diffraction points of GaN and GaAs, which is in excellent agreement with the reported value [19].

The TEM micrograph in Fig. 4(b) reveals structural details at the GaN/GaAs interface. Stacking faults were identified from the interface, which are presumably originated by the lattice mismatch. These planar defects are characterized by pyramid structures along the (1 $\bar{1}$ 1) and ($\bar{1}$ 1 1) planes with an inclination angle of 54.7° respect to the (0 0 1) substrate surface. It is important to emphasize that in the first nanometers of growth, the sample presents purity of cubic phase, indicating that the hexagonal component is not formed from the interface, in contrast to results from other

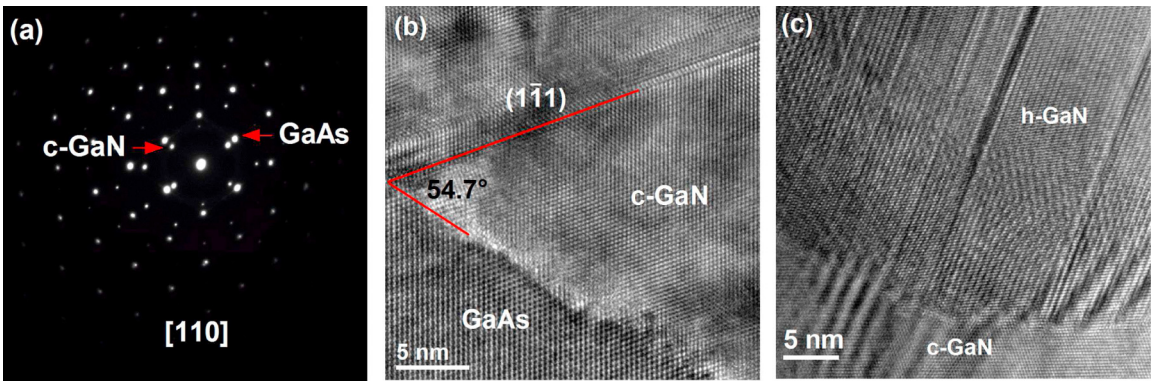

Fig. 4. (a) SAD patterns taken along [1 1 0] direction at the interface, for sample IV. Cross-sectional HR-TEM micrograph of: (b) GaN/GaAs interface showing stacking faults and, (c) detail of hexagonal inclusions of GaN, for sample IV.

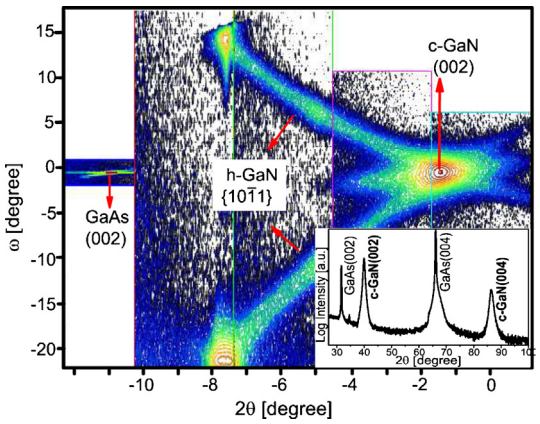

Fig. 5. X-ray RSM of the c-GaN(0 0 2) and h-GaN {1 0 $\bar{1}$ 1} planes for sample II, along the azimuth angle $\varphi = 0^\circ$. The inset shows the $\theta - 2\theta$ X-ray diffraction curve from this sample.

groups [9]. These results suggest that the As_4 overpressure during the nucleating layer allowed the growth of predominantly the cubic phase, reiterating its importance during this stage. Nevertheless, we found hexagonal inclusions after the several nanometers of growth, as shown in the micrograph of Fig. 4(c). We attribute the origin of these components at stacking faults, since one hexagonal monolayer can be considered as one stacking fault. A discussion about these planar defects in our c-GaN samples was performed by Ruiz-Zepeda et al. [20].

Now we want to highlight some characteristics of the c-GaN layers, such as the crystalline quality and cubic phase purity. The full-width at half maximum (FWHM) of the ω-scan of the cubic GaN samples are shown in Table 1. X-ray RSM was used to obtain information on the content of hexagonal inclusions and their distribution [21,22]. In order to obtain an accurate estimate of the component, the measurements were made along the azimuth angles $\varphi = 0^\circ$, $\varphi = 90^\circ$, $\varphi = 180^\circ$ and $\varphi = 270^\circ$. Fig. 5 shows X-ray RSM along $\varphi = 0^\circ$ for sample II of Table 1. The hexagonal inclusions were found on the {1 1 1} planes, as previously discussed in Fig. 4 and reported by Ruiz-Zepeda et al. [20]. The h-GaN component was calculated by comparing the integrated X-ray diffraction intensity of the cubic (0 0 2) and hexagonal (1 0 $\bar{1}$ 1) planes, in the same diffraction volume, more details of the calculation procedure can be found in Ref. [23]. The RSM quantification demonstrated that the GaN samples have a high purity of cubic phase. In fact, the $\theta - 2\theta$ diffraction pattern showed only the diffraction peaks associated to (0 0 2) and (0 0 4) planes of GaAs and c-GaN, as can be observed in the inset of Fig. 5.

Fig. 6(a) presents the calculated percentage of hexagonal components performed for azimuth angles φ along the $\{1\,1\,1\}_N$ and $\{1\,1\,1\}_{Ga}$ planes of c-GaN as a function of the As_4 overpressure exposure time (τ_{As_4}). We found a smaller hexagonal component on the $\{1\,1\,1\}_N$ planes. The fine details in the hexagonal content appreciated on the planes $\{1\,1\,1\}_N$ and $\{1\,1\,1\}_{Ga}$, suggest that the growth mechanism is different on the {1 1 1} planes of the c-GaN. Fig. 6(b) schematically illustrates (1 1 1) and ($\bar{1}$ $\bar{1}$ 1) planes, which are terminated with Ga atoms. Fig. 6(c) shows (1 $\bar{1}$ 1) and ($\bar{1}$ 1 1) planes, which are terminated with N atoms [24]. The difference in the amount of hexagonal inclusions observed along the azimuths could be due to the different intrinsic properties of the Ga and N bonds on each plane.

It is well known that the chemical nature of the surface atoms is crucial for the III-nitrides epitaxial growth. In particular, under Ga-rich condition, Ga adatoms have a higher mobility and thus the samples synthesize with better crystalline quality [25]. Note that in our samples we employed a Ga-rich growth condition. On the other hand, a higher growth rate on $(1\,1\,1)_{Ga}$ and $(\bar{1}\,\bar{1}\,1)_{Ga}$ planes has been reported, compared to that on $(1\,\bar{1}\,1)_N$ and $(\bar{1}\,1\,1)_N$ planes [26]. In this case, the highly mobile Ga adatoms on $(1\,\bar{1}\,1)_N$ and $(\bar{1}\,1\,1)_N$ planes have a higher probability to find appropriate surface sites before being incorporated in the lattice, reducing the density of stacking faults and therefore the hexagonal component on these planes. RHEED patterns taken during the GaN growth also evidenced the difference in the hexagonal inclusions along the [1 1 0] and [1 $\bar{1}$ 0] directions. The streaky and bright pattern along [1 1 0] direction shown in the inset of Fig. 6(a) clearly presents a 2x surface reconstruction indicating a smooth surface. In contrast, RHEED pattern along [1 $\bar{1}$ 0] direction presents some spotty features coming from the hexagonal component.

We found that the relaxation process of c-GaN, which starts at the stage II (τ_{II}) of Fig. 2, affects the purity of cubic phase. The sample II presented the higher purity of cubic phase, as shown in Fig. 6(a). This sample initiated the relaxation process at $\tau_{II} = 22$s (Table 1), which corresponds approximately to 8ML. Thus, these few monolayers grown under As_4 overpressure are able to promote a stable nucleating layer. If we chose growth parameters that promotes a rapid relaxation process, for example, sample I ($\tau_{II} = 4.5$s), with a short As_4 overpressure of 3s, the hexagonal incorporation increased

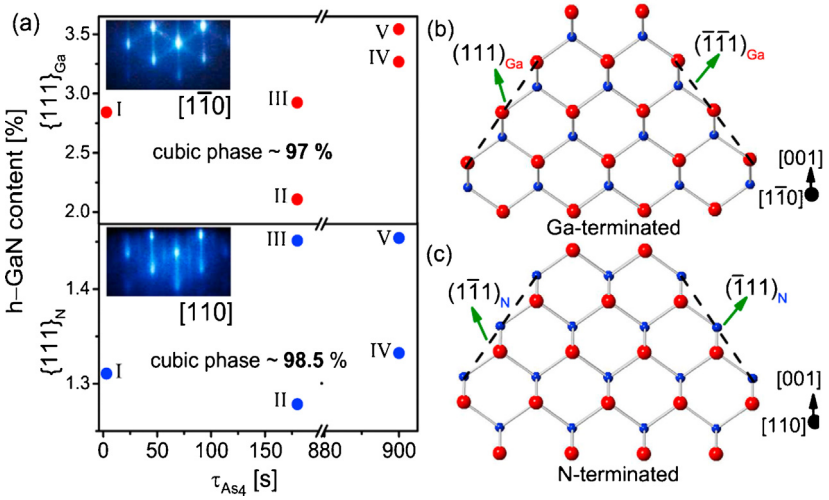

Fig. 6. (a) Hexagonal inclusions in the c-GaN samples grown at different As_4 exposure time (τ_{As_4}), for azimuth angles along the $\{1\,1\,1\}_N$ and $\{1\,1\,1\}_{Ga}$ planes. Schematic picture of (b) $(1\,1\,1)_{Ga}$ and $(\bar{1}\,\bar{1}\,1)_{Ga}$ planes, and (c) $(1\,\bar{1}\,1)_N$ and $(\bar{1}\,1\,1)_N$ planes of the c-GaN.

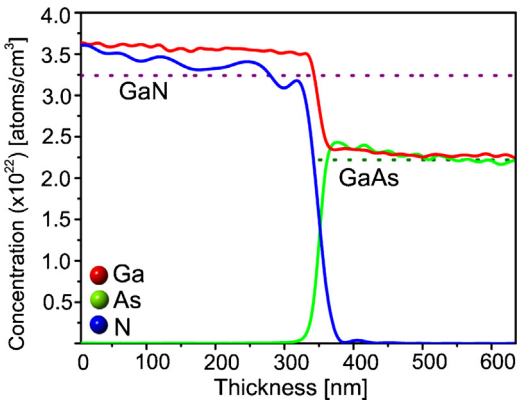

Fig. 7. SIMS depth profiles for Ga (red), As (green), and N (blue) for sample II. (For interpretation of the references to color in this figure legend, the reader is referred to the web version of this article.)

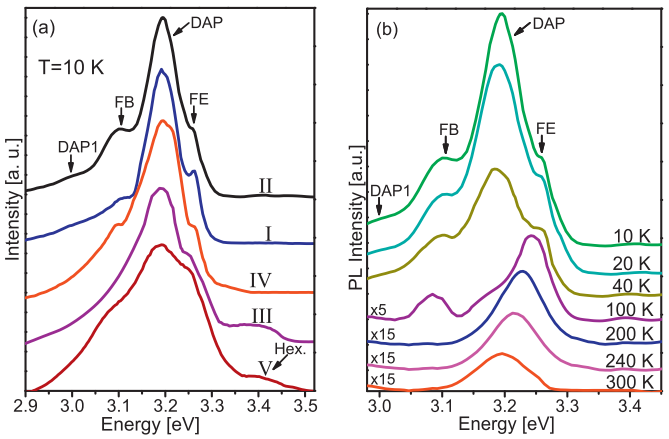

Fig. 8. (a) PL spectra from cubic GaN samples I–V (see Table 1), measured at 10K. (b) PL spectra for sample II, measured at different temperatures.

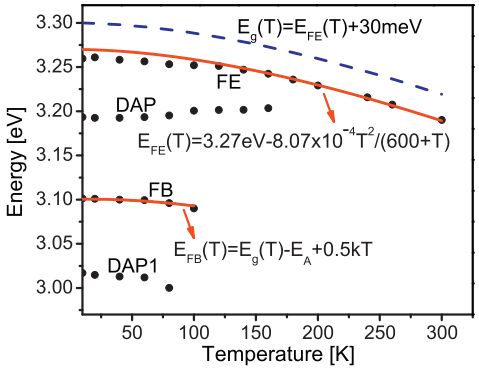

Fig. 9. Temperature dependence of the PL peak energies of the FE, DAP, FB and DAP1 for sample II.

(see Fig. 6(a)). In this case, the fast relaxation process induces a layer with crystal defects that are propagated along the growth. On the other hand, we observed that the sample III presented a higher hexagonal inclusions compared to the sample II. This is due to the lower growth temperature T_{GL} after the nucleating layer for this sample (710°C). That is, the higher T_{GL} for sample II leads to a higher desorption of As and Ga, which forms a stable layer that promotes the growth of the cubic phase. Likewise, the relaxation process for sample IV is similar to the sample II. Nevertheless, the sample II presents a higher purity of cubic phase. For sample IV, the prolonged As exposure ($\tau_{As_4} = 900$ s) after the formation of the stable layer affects the dynamic of growth, in such way that it induces the density of planar defects, and hexagonal inclusions. The highest purity of 98.7% of cubic phase was obtained for sample II on the $\{1\,1\,1\}_N$ planes and 97.9% on the $\{1\,1\,1\}_{Ga}$ planes. This sample presents the narrowest FWHM of the ω-scan as shown in Table 1.

Despite the differences of the growth on the $\{1\,1\,1\}$ planes, we have been able to achieve c-GaN films with an uniform distribution of Ga and N within the bulk, as shown in Fig. 7 by SIMS depth profile measurements. The analyzed area was 100μm^2 and sputtered with oxygen over an square area of 300μm^2. Moreover, the signals from As also allow us to ensure that As atoms are confined at the interface GaN/GaAs.

The design of new devices with c-GaN requires high purity of cubic phase with appropriated physical properties. Having achieved a high degree of phase purity as was previously discussed, now we show the photoluminescence properties of the samples. PL spectra measured at 10K from samples I–V are shown in Fig. 8(a). In all samples, we found four resolved peaks assigned to free exciton (FE), donor-acceptor pair (DAP), free electron to acceptor (FB) and DAP1 transitions in c-GaN, [27,28]. The samples IV and V presented a wider FWHM of the DAP peak, probably by the prolonged As_4 overpressure ($\tau_{As_4} = 900$ s). Moreover, we identified an additional small peak at 3.38eV related to hexagonal inclusions for samples III and V, these samples present the higher content of hexagonal inclusions (see Fig. 6). PL spectra for sample II measured at different temperatures are shown in Fig. 8(b). As the temperature increases, the intensity from the FE peak increases in relation to the DAP emission, and above 160K the FE peak dominates the PL emission. The FWHM of the FE peak at room temperature is 94meV.

For clarity PL peak energies for sample II as a function of temperature are shown in Fig. 9. The temperature dependence of the FE peak was fitted by using Varshni's empirical equation [29]. We found at low temperatures that the fit curve deviates from the FE peak by 10meV. This deviation is consequence of the contribution of the bound exciton transition, which has been widely discussed [30]. The temperature dependence of the band gap is described by $E_g(T) = E_{FE}(T) + 30$meV, where $E_{FE}(T)$ is the temperature variation of the FE peak and 30meV is the binding energy of FE transition, as shown in Fig. 9 by dashed line. Regarding the DAP transition, we found that at 10K, the emission is about of 3.19eV which could be due to the high residual donor carrier concentration ($\sim 10^{19}$cm^{-3}). We observe that this emission shifts toward higher energies by increasing temperature. The DAP1 peak shifts to lower energies by increasing the temperature. The different behavior of these transitions could indicate that the acceptors involved in DAP and DAP1 transitions are of different nature [27,29,31]. Finally for the FB emission, the PL peak moves toward lower energy with increasing temperature, which is consistent with the temperature dependence of $E_g(T)$ [27], as shown in Fig. 9.

4. Conclusions

We have grown c-GaN on GaAs (0 0 1) substrates by using an As_4 overpressure during the nucleating layer. Our results showed that the relaxation process of c-GaN during the nucleating layer affects the cubic phase purity. A rapid starting of the relaxation process of c-GaN (for example 4.5s in sample I) generates a nucleating layer with defects, such as hexagonal inclusions, that are propagated along the growth. In contrast, the samples present a higher purity of cubic phase, when the relaxation process is initiated after several monolayers of growth (for example 8 ML that corresponds to 22s in sample II). This slower relaxation process is a result of increasing the interval of time of As_4 overpressure exposure. The presence of As atoms on the growth surface is limited by increase in the growth temperature after the nucleating layer, that promotes

the desorption of this element. It is important to emphasize that the grown samples presented a high purity of cubic phase reiterating the importance of the As_4 overpressure during the nucleating process. Hexagonal components are formed from stacking faults after several nanometers of growth. In the estimation of the hexagonal inclusions by RSM, we found fine details on the {1 1 1} planes. Higher purity of cubic phase was obtained on $(1\,\bar{1}\,1)_N$ and $(\bar{1}\,1\,1)_N$ planes, compared to the $(1\,1\,1)_{Ga}$ and $(\bar{1}\,\bar{1}\,1)_{Ga}$ planes. At low temperatures the PL measurements showed transitions associated with bound-exciton, donor–acceptor pairs, and free electron to acceptor from c-GaN. At room temperature the free exciton emission dominated the PL spectra, indicative of high purity of cubic phase. In samples with higher hexagonal content we detected an PL emission of a small peak from hexagonal inclusion.

Acknowledgements

This work was partially supported by CONACyT-SENER Project No. 151076. The authors would like to thank A. Tavira, A. Guillén, D.A. Flores-Cordero, A.B. Soto and M. Guerrero for their technical assistance.

References

[1] S. Nakamura, M. Senoh, S. Nagahama, N. Iwasa, T. Yamada, T. Matsushita, H. Kiyoku, Y. Sugimoto, T. Kozaki, H. Umemoto, M. Sano, K. Chocho, Continuous-wave operation of InGaN/GaN/AlGaN-based laser diodes grown on GaN substrates, Appl. Phys. Lett. 72 (16) (1998) 2014–2016.
[2] J.W. Orton, C.T. Foxon, Group III nitride semiconductors for short wavelength light-emitting devices, Rep. Prog. Phys. 61 (1998) 1–75.
[3] D.J. As, in: M.O. Manasreh (Ed.), Optoelectronic Properties of Semiconductors and Superlattices, vol. 19, Taylor & Francis Books, Inc., New York, 2003, chapter 9.
[4] D.J. As, Recent developments on non-polar cubic group III-nitrides for optoelectronic applications, Proc. SPIE 7608 (2010), 76080G1-76080G15.
[5] S.V. Novikov, C.T. Foxon, A.J. Kent, Zinc-blende (cubic) GaN bulk crystals grown by molecular beam epitaxy, Phys. Status Solidi C 8 (5) (2011) 1439–1444.
[6] H. Vilchis, V.M. Sanchez-R, A. Escobosa, Cubic GaN layers grown by metalorganic chemical vapor deposition on GaN templates obtained by nitridation of GaAs, Thin Solid Films 520 (2012) 5191–5194.
[7] O. Ambacher, J. Majewski, C. Miskys, A. Link, M. Hermann, M. Eickhoff, M. Stutzmann, F. Bernardini, V. Fiorentini, V. Tilak, B. Schaff, L.F. Eastman, Pyroelectric properties of Al(In)GaN/GaN hetero- and quantum well structures, J. Phys.: Condens. Matter 14 (2002) 3399–3434.
[8] G. Ramírez-Flores, H. Navarro-Contreras, A. Lastras-Martínez, R.C. Powell, J.E. Greene, Temperature-dependent optical band gap of the metastable zinc-blende structure β-GaN, Phys. Rev. B 50 (12) (1994) 8433–8438.
[9] D.J. As, T. Frey, D. Schikora, K. Lischka, V. Cimalla, J. Pezoldt, R. Goldhahn, S. Kaiser, W. Gebhardt, Cubic GaN epilayers grown by molecular beam epitaxy on thin β-SiC/Si(0 0 1) substrates, Appl. Phys. Lett. 76 (13) (2000) 1686–1688.
[10] M.J. Paisley, Z. Sitar, J.B. Posthill, R.F. Davis, Growth of cubic phase gallium nitride by modified molecular-beam epitaxy, J. Vac. Sci. Technol. A 7 (3) (1989) 701–705.
[11] K.H. Ploog, O. Brandt, H. Yang, B. Yang, A. Trampert, Nucleation and growth of GaN layers on GaAs, Si, and SiC substrates, J. Vac. Sci. Technol. B 16 (4) (1998) 2229–2236.
[12] B. Daudin, G. Feuillet, J. Hübner, Y. Samson, F. Widmann, A. Philippe, C. Bru-Chevallier, G. Guillot, E. Bustarret, G. Bentoumi, A. Deneuville, How to grow cubic GaN with low hexagonal phase content on (0 0 1) SiC by molecular beam epitaxy, J. Appl. Phys. 84 (4) (1998) 2295–2300.
[13] J. Wu, H. Yaguchi, K. Onabe, Y. Shiraki, R. Ito, Metalorganic vapor phase epitaxy growth of high quality cubic GaN on GaAs (1 0 0) substrates, Jpn. J. Appl. Phys. 37 (3B) (1998) 1440–1442.
[14] T.S. Cheng, L.C. Jenkins, S.E. Hooper, C.T. Foxon, J.W. Orton, D.E. Lacklison, Selective growth of zinc-blende, wurtzite, or a mixed phase of gallium nitride by molecular beam epitaxy, Appl. Phys. Lett. 66 (12) (1995) 1509–1511.
[15] O. Zsebök, J.V. Thordson, J.R. Gunnarsson, Q.X. Zhao, L. Ilver, T.G. Andersson, The effect of the first GaN monolayer on the nitridation damage of molecular beam epitaxy grown GaN on GaAs (0 0 1), J. Appl. Phys. 89 (7) (2001) 3662–3667.
[16] S. Gwo, H. Tokumoto, S. Miwa, Atomic-scale nature of the (3×3)-ordered GaAs(0 0 1):N surface prepared by plasma-assisted molecular-beam epitaxy, Appl. Phys. Lett. 71 (3) (1997) 362–364.
[17] S. Naritsuka, M. Mori, Y. Takeuchi, Y. Monno, T. Maruyama, XPS study of nitridation mechanism of GaAs(0 0 1) surface by RF-radical source, Phys. Status Solidi C 8 (2) (2011) 291–293.
[18] A. Trampert, O. Brandt, H. Yang, K.H. Ploog, Direct observation of the initial nucleation and epitaxial growth of metastable cubic GaN on (0 0 1) GaAs, Appl. Phys. Lett. 70 (5) (1997) 583–585.
[19] D. Chandrasekhar, D.J. Smith, S. Strite, M.E. Lin, H. Morkoç, Characterization of Group III-nitride semiconductors by high-resolution electron microscopy, J. Cryst. Growth 152 (3) (1995) 135–142.
[20] F. Ruiz-Zepeda, Y.L. Casallas-Moreno, J. Cantu-Valle, D. Alducin, U. Santiago, M. José-Yacaman, M. López-López, A. Ponce, Precession electron diffraction-assisted crystal phase mapping of metastable c-GaN films grown on (0 0 1) GaAs, Microsc. Res. Tech. 77 (12) (2014) 980–985.
[21] B. Qu, X. Zheng, Y. Wang, Z. Feng, J. Han, S. Liu, S. Lin, H. Yang, J. Liang, Multiplicity factor and diffraction geometry factor for single crystal X-ray diffraction analysis and measurement of phase content in cubic GaN/GaAs(0 0 1) epilayers, Sci. China (Ser. A) 44 (4) (2001) 497–503.
[22] Z.Q. Li, H. Chen, H.F. Liu, J.H. Li, L. Wan, S. Liu, Q. Huang, J.M. Zhou, MBE growth and X-ray study of high-quality cubic-GaN on GaAs(0 0 1), J. Cryst. Growth 208 (2000) 786–790.
[23] Y.L. Casallas-Moreno, M. Pérez-Caro, S. Gallardo-Hernández, M. Ramírez-López, I. Martínez-Velis, A. Escobosa-Echavarría, M. López-López, Study of structural properties of cubic InN films on GaAs(0 0 1) substrates by molecular beam epitaxy and migration enhanced epitaxy, J. Appl. Phys. 113 (21) (2013), 214308(1)-214308(5).
[24] Z.X. Qin, H. Nagano, Y. Sugure, A.W. Jia, M. Kobayashi, Y. Kato, A. Yoshikawa, K. Takahashi, High-resolution X-ray diffraction analysis of cubic GaN grown on (0 0 1)GaAs by RF-radical source molecular beam epitaxy, J. Cryst. Growth 189/190 (1) (1998) 425–429.
[25] P. Ruterana, M. Albrecht, J. Neugebauer, Nitride Semiconductors: Handbook on Materials and Devices, Wiley-VCH, 2003.
[26] B. Qu, X.H. Zheng, Y.T. Wang, S.M. Lin, H. Yang, J.W. Liang, Polarity dependence of hexagonal inclusions and cubic twins in GaN/GaAs(0 0 1) epilayers measured by conventional X-ray pole figure and grazing incident diffraction pole figure, J. Cryst. Growth 226 (1) (2001) 57–61.
[27] D. Xu, H. Yang, J.B. Li, D.G. Zhao, S.F. Li, S.M. Zhuang, R.H. Wu, Y. Chen, G.H. Li, Optical characterization of high-purity cubic GaN grown on GaAs (0 0 1) substrate by metalorganic chemical vapor deposition, Appl. Phys. Lett. 76 (21) (2000) 3025–3027.
[28] S. Strite, J. Ruan, Z. Li, A. Salvador, H. Chen, D.J. Smith, W.J. Choyke, H. Morkoç, An investigation of the properties of cubic GaN grown on GaAs by plasma-assisted molecular-beam epitaxy, J. Vac. Sci. Technol. B 9 (4) (1991) 1924–1929.
[29] S.J. Xu, C.T. Or, Q. Li, L.X. Zheng, M.H. Xie, S.Y. Tong, H. Yang, Defect states in cubic GaN epilayer grown on GaAs by metalorganic vapor phase epitaxy, Phys. Status Solidi (a) 188 (2) (2001) 681–685.
[30] Z.X. Liu, A.R. Goñi, K. Syassen, H. Siegle, C. Thomsen, B. Schöttker, D.J. As, D. Schikora, Pressure and temperature effects on optical transitions in cubic GaN, J. Appl. Phys. 86 (2) (1999) 929–934.
[31] J. Wu, H. Yaguchi, K. Onabe, R. Ito, Y. Shiraki, Photoluminescence properties of cubic GaN grown on GaAs(1 0 0) substrates by metalorganic vapor phase epitaxy, Appl. Phys. Lett. 71 (15) (1997) 2067–2069.